

## Sustained JNK1 activation is associated with altered histone H3 methylations in human liver cancer <sup>☆,☆☆</sup>

Qingshan Chang<sup>2</sup>, Yadong Zhang<sup>1</sup>, Kevin J. Beezhold<sup>1,3</sup>, Deepak Bhatia<sup>1</sup>, Hongwen Zhao<sup>1,4</sup>, Jianguo Chen<sup>5</sup>, Vince Castranova<sup>1</sup>, Xianglin Shi<sup>1,2</sup>, Fei Chen<sup>1,2,3,\*</sup>

<sup>1</sup>The Health Effects Laboratory Division, National Institute for Occupational Safety and Health, Pathology and Physiology Research Branch, 1095 Willowdale Road, Morgantown, WV 26505, USA

<sup>2</sup>Graduate Center for Toxicology, University of Kentucky, Lexington, KY 40536, USA

<sup>3</sup>Cancer Cell Biology Program, West Virginia University, Morgantown, WV 26506, USA

<sup>4</sup>Institute of Respiratory Diseases, First Affiliated Hospital, China Medical University, Shenyang 110001, PR China

<sup>5</sup>Qidong Liver Cancer Institute, Jiangsu Province, Qidong 226200, PR China

**Background/Aims:** Aberrant c-Jun N-terminal kinase (JNK) activation has been linked to hepatocellular carcinoma (HCC) in mouse models. It remains unclear whether JNK activation plays an important role in human HCC and, if so, how JNK signaling contributes to the initiation or progression of HCC.

**Methods:** The JNK activation, global gene expression, and the status of histone H3 methylations were measured in 31 primary human hepatocellular carcinoma (HCC) samples paired with the adjacent non-cancerous (ANC) tissues.

**Results:** Enhanced JNK1 activation was noted in 17 out of 31 HCC samples (55%) relative to the corresponding ANC tissues, whereas JNK2 activation was roughly equal between HCC and ANC tissues. This enhancement in JNK1 activation is associated with an increased tumor size and a lack of encapsulation of the tumors. In addition, an association of JNK1 activation with the histone H3 lysines 4 and 9 tri-methylation was observed in the HCC tissues, which leads to an elevated expression of genes regulating cell growth and a decreased expression of the genes for cell differentiation and the p450 family members in HCC.

**Conclusions:** These results, thus, suggest that JNK1 plays important roles in the development of human HCC partially through the epigenetic mechanisms.

Published by Elsevier B.V. on behalf of the European Association for the Study of the Liver.

**Keywords:** JNK; HCC; H3K4me3; EZH2; Tumor suppressor

Received 23 April 2008; received in revised form 7 July 2008; accepted 23 July 2008; available online 16 October 2008

Associate Editor: J.M. Llovet

\* NIH funded study (Grants 5R01CA119028 and 5R01CA116697). The authors declare that they do not have anything to disclose regarding funding from industries or conflict of interest with respect to this paper.

<sup>☆☆</sup> **Disclaimer:** The opinions expressed in this manuscript are those of the authors and do not necessarily represent the views of the National Institute for Occupational Safety and Health, Center for Disease Control and Prevention of the USA.

\* Corresponding author. Tel.: +1 304 285 6021.

E-mail address: LFD3@cdc.gov (F. Chen).

**Abbreviations:** HCC, hepatocellular carcinoma; JNK, C-Jun N-terminal kinase; H3K4me3, histone H3 lysine 4 tri-methylation; C-CNB1, cyclin B1; CCNA, cyclin A2; CDC2, cell division cycle protein 2.

### 1. Introduction

Human hepatocellular carcinoma (HCC) accounts for about 618,000 cancer deaths worldwide annually, which represents the third leading cause of cancer death [1–3]. In Eastern Asia and Central Africa, HCC has accounted for nearly 70% of cancer deaths [4]. In the last two decades, a remarkable increase in HCC incidence has also been noted in Europe and the United States [5]. The most common etiology of human HCC is chronic hepatitis resulting from HBV (mainly in Asia and Africa) or HCV (more frequently in the West) infection [1,5]. Additional risk factors for HCC are non-alcoholic fatty liver

disease, environmental pollutants including arsenic, aflatoxin B1, aromatic amines, vinyl chloride, polycyclic aromatic hydrocarbons, and nitrosamines [2,6]. Despite the enormous efforts that has been made, the molecular mechanism underlying the initiation and progression of HCC is still only poorly understood. It is generally accepted that tumorigenesis in the liver results from a progressive genetic alterations that promote the malignant transformation of hepatocytes by disrupting processes important for cell cycle, apoptosis, and differentiation. Indeed, a recent study employing an integrative oncogenomic approach suggested that genomic amplification of cIAP1 and Yap plays a pivotal role on the sustained rapid growth of liver tumors [7]. Furthermore, a subset of HCC signature genes has been identified by gene expression profiling among patients with varied levels of serum  $\alpha$ -fetoprotein [8]. All of these HCC signature genes are capable of contributing to active metabolism and growth regulation of hepatocytes.

In addition to genomic abnormalities, aberrant signaling networks that link to intracellular kinase activation or activity have been frequently observed in a considerable number of experimental systems. In animal models, several recent studies suggested that kinase activation or deficiency, such as c-Jun N-terminal kinase (JNK) and I $\kappa$ B kinase (IKK), plays a major role in the clonal expansion and proliferation of the hepatocytes [9–11]. JNK was initially identified as a protein kinase in the liver of rodents exposed to cycloheximide [12]. At least 10 JNK isoforms are produced by alternative splicing of mRNAs transcribed from JNK1, JNK2, and JNK3 genes [13]. Although JNK was predominantly involved in cellular stress responses, emerging evidence supports a role for JNK in cell proliferation and tumorigenesis. Hepatocytes express both JNK1 and JNK2 that are functionally overlapping in response to diverging stress or growth signals. However, non-redundant roles of JNK1 and JNK2 have been demonstrated in experiments using JNK1 and JNK2 gene knockout mice or the cells derived from these animals [14]. JNK1, rather than JNK2, appears to be the key kinase responsible for TNF $\alpha$ -induced c-Jun phosphorylation, cell proliferation and BCR/Abl-mediated transformation of pre-B cells [14,15]. A sustained JNK1 activation has been linked to chemical carcinogen-induced HCC in mice with hepatocyte-specific gene knockout of IKK $\beta$ , an upstream kinase for NF- $\kappa$ B activation [11]. It is unknown whether these animal models are representative of human HCC, however, since there are no data currently available that indicate alterations in the activation and activity of these kinases in the development of human HCC. In the present report, we revealed that human HCC exhibited an increased activation of JNK1 relative to the paired adjacent non-cancerous (ANC) tissues, whereas equal levels of JNK2 activation were observed between HCC and non-cancerous tissues. We also showed that JNK1 activation is asso-

ciated with an up-regulation of histone H3 lysine 4 trimethylation (H3K4me3), thereby increasing expression of genes contributing to cell mitosis, metabolism and biogenesis. In addition, an inverse relationship between JNK1 activation and the expression of the genes for cell differentiation, p450 members and redox regulation was observed in the primary HCC samples.

## 2. Materials and methods

### 2.1. Collection of tissue samples

The HCC tissue samples along with the adjacent non-cancerous (ANC) tissues were obtained from surgical resections of liver tumors with informed consent of the patients according to the approved protocol of the institutional review board at Qidong Liver Cancer Institute, PR China. HCC was diagnosed according to EASL guidelines [4]. Clinical or pathological stage was determined using Okuda score systems [16]. Demographic data of the patients were indicated in Table 1 and Supplemental Table 1. The tissue samples were numerically labeled based on the date of collection, such as 1, 2, or 3. All samples were histopathologically examined and classified based on criteria outlined by the Liver Cancer Study Group of Japan [17]. Tumor volume (cm<sup>3</sup>) was determined by measuring the length (*L*), width (*W*), and thickness (*T*) of the resected tumors and calculated as  $L \times W \times T$ .

### 2.2. Western blotting

Total tissue lysates were prepared using RIPA buffer for Western blotting. The tissue lysates were separated by SDS-PAGE and transferred to nitrocellulose membranes that were immunoblotted with antibodies against phospho-JNK, total JNK, H3K4me1, H3K4me3, H3K9me3, H3K9me36, and  $\alpha$ -tubulin. Specific antibodies for JNK1 and JNK2 were purchased from Santa Cruz Biotechnology (Santa Cruz, CA) and Cell Signaling Technology (MA), respectively. The antibodies against methylated histones were purchased from Abcam Inc. (MA). Quantification of the Western blotting was made by using AlphaEase software version 5.5 (Alpha Innotech Corporation, San Leandro, CA). In some experiments, the mouse embryo stem cell (ES) lines derived from wild-type or SEK1 knockout E14K ES cells, gifts of Dr. Hiroshi Nishina at University of Tokyo, were used for protein preparation. The cells were maintained in complete DMEM containing 15% fetal calf serum. The differentiation of ES cells was prevented by passing the cells every 2 or 3 days and by supplying the cells with 1000 U/ml of ESGRO (Chemicon, Temecula, CA).

**Table 1**  
Demographic data of the HCC patients.

	Number of patients
Total number of patients	31
Male/female	23/8
Age (mean/range)	53 (32–74)
AFP (–/ <100/100–400/>400)	7/8/4/12
HBV (+/–)	22/9
Family HCC history (Yes/No)	13/18
Tumor size (mean/range cm <sup>3</sup> )	146 (8–504)
Encapsulation (+/–)	15/16
Tumor grade (II/III)	14/17
Cirrhosis (+/–)	14/17
Liver inflammation (+/–)	26/5

2.3. RT-PCR

For traditional RT-PCR, 1 µg of total RNA was used for each reaction of RT-PCR with a temperature scale of 40 °C for 50 min for reverse transcription, and 25 cycles of 94 °C for 30 s, 56 °C for 1 min 30 s, and 72 °C for 1 min 30 s. For the purpose of verification, a quantitative real-time RT-PCR was performed as reported previously [18]. Data show mRNA expression levels relative to those of GAPDH. The PCR primers are:

Gene names	Sense (5' -> 3')	Antisense (5' -> 3')
MAP3K7	ATGTCTACAGCCTCTGCCGC	GCTCTGTCCTTCATCTGAATACTGAC
MAP3K13	TTTATTTTACCACGTGGGATGCAT	ACAGGGTTGTTGTGAGGATCATAATG
MAP4K3	CACTGGTGAATTAGCAGCAATTAAG	CGATTGCCAAAGACCGTGTCAAATG
MAPK9	ATGAGCGACAGTAAATGTGACAGTC	CTTCCAACCTGGGCATCATAAATTTG
PBK	ATGGAAGGGATCAGTAATTTCAAGAC	CTAGACATCTGTTTCCAGAGCTTCA
RHAMM	GATGAGGGGTATGATGGCTAAGCA	TAACGCTTTATAGCTTTCAAATTGAG
SMYD3	TCTTGGCAGAGTTGTCTTCAAACCTA	TTAGGATGCTCTGATGTTGGCGTC
SMYD5	TTGGCAGCCACTGAGCAATAC	CACACATCAGTCATCTCATCCCCAG
STAB2	TACAATTAGGACCGAGTGCCGAT	GCAAATGCATTTCAGTTCGGCCTG
EZH2	TGTGGACCACAGTGTTACCAGCAT	ATGGCTCTCTGGCAAAAATACCT
IKKα	ACGTCTGTCTGTACCAGCATCG	ATTTATTCCAGTTTCACGCTCA
IKKβ	GGTGAGCAGATTGCCATCAAG	ACCCTCAGTTCGCTGGTCTCG
NEMO	AGGACGTAAGGGCGAAGAGT	GGAACGGTCTCCATCACAATC
GAPDH	CTCAGACACCATGGGGAAGGTGA	ATGATCTTGAGGCTGTTGTCATA

products to lengths of 35–200 bp, the cRNAs were added to a solution at a final cRNA concentration of 50 µg/ml for hybridization to Affymetrix GeneChip HG-U133 plus 2 oligonucleotide microarray chips. Following hybridization the microarrays were washed, stained, and scanned. Genechip Operating Software v1.4 (Affymetrix, Santa Clara, CA) was used to extract images. The raw chip data were normalized by using GeneSpring software 7.3.1 (Agilent Technologies, Waldbronn, Germany).

2.4. Chromatin immunoprecipitation (ChIP)

ChIP assays were performed according to the protocol from Chromatin Immunoprecipitation Kit (Upstate Technology, Lake Placid, NY). Briefly, 100 µg of each sample tissue was selected and cut into fine pieces. Then the samples were cross-linked with 1% formaldehyde for 10 min and subjected to 10 sonication cycles for shearing cross-linked DNA to 200–1200 bp in length [30 s sonication in an Ultrasonic Processor (Dr. Hielscher) at 90 W, followed by a 2 min rest on ice]. One hundred microliter of aliquot was then incubated with anti-H3K4me3 (4 µg, Abcam, # ab8580), or 5 µg of normal rabbit IgG, as a negative control. Semi-quantitative PCRs were performed with ChIP-bound and input DNA, respectively, using following primers:

CCNB1	GCTGCTACCGTAGAAATGGAAAGTG	GCCACAGTGAGGCTAGGCCG
CCNA2	GGAAAAAGTCACTTAAGCTAACTAG	CAAGTATCCCGCGACTATTGAAATG
CDC2	AGAAGAACGGAGCGAACAGTAGC	GTTTCAAACCTCACCGCGCTAAAG
CDC25C	AGAGGGAGAGCCAATGATGCGC	TGACCATTCAAACCTTCCGCCAG
CCNB1ORF	ATGGGAAGGGAGTGAGTGCCACG	AGCAGGCAGCAGCTAAGAAGGC
CCNA2ORF	CTATTCTTTGGCCGGTTCGGT	TCTTCGGCCTCTGCTGCTGC
CDC2ORF	CTTTAGCGCGGTGAGTTTGAAC	AGTGTGGCTACACGGCCAGA
CDC25CORF	TGGCTGACGCAGCTTAGAGGC	GGAGAGAAAGTAGATAGGGATCGGAC

2.5. Gene expression profiling

Total RNA was extracted from frozen HCC tissue samples and the paired non-cancerous tissues (ANC) using TRIzol reagent according to the manufacturers' suggestion (Invitrogen). The RNA was then cleaned up using RNEasy midi-columns (Qiagen, Chatsworth, CA). The integrity of RNA from each sample set was confirmed with the Agilent 2100 Bioanalyzer (Agilent Technologies, Palo Alto, CA). The labeling and the hybridization of mRNAs were performed according to Affymetrix One-Cycle Target Labeling protocols (<http://www.affymetrix.com/support/developer/tolls/affytools.affx>). Briefly, 5 µg of total RNA was reverse transcribed with a T7-oligo (dT)24 primer and the Superscript II reverse transcriptase (Invitrogen). Second-strand synthesis was followed by cRNA generation with incorporation of biotinylated ribonucleotides. After fragmentation of the cRNA

2.6. Statistics and criteria of significance

To generate gene lists, log transformed data were compared between groups using Welch's *T*-test with Bonferroni correction and median normalization. Signal values were evaluated with the scale: a signal log ratio of 1.0 indicating an increase of the transcript level by 2-fold and -1.0 indicating a decrease by 2-fold, and signal log ratio of zero meaning no change.

A *p*-value cut-off of <0.05 and a fold change difference of ≥2 in all analyzed samples were considered to be significant. Other quantitative data were analyzed by using SigmaPlot 9.0 statistics software. Data are expressed as means ± standard deviations. The Fisher's exact test was used to analyze the statistic difference of the absence of encapsulation

of the tumors between groups showed in Fig. 1D. The representative data of RT-PCR and Western blotting are derived from at least three replications.

3. Results

3.1. JNK1 activation associates with HCC tumor size

We collected 31 HCC tissue samples during 2004 and 2005 for the present studies. The partial clinical characteristics of these patients are summarized in Table 1. To determine the state of kinase activity in human HCC,

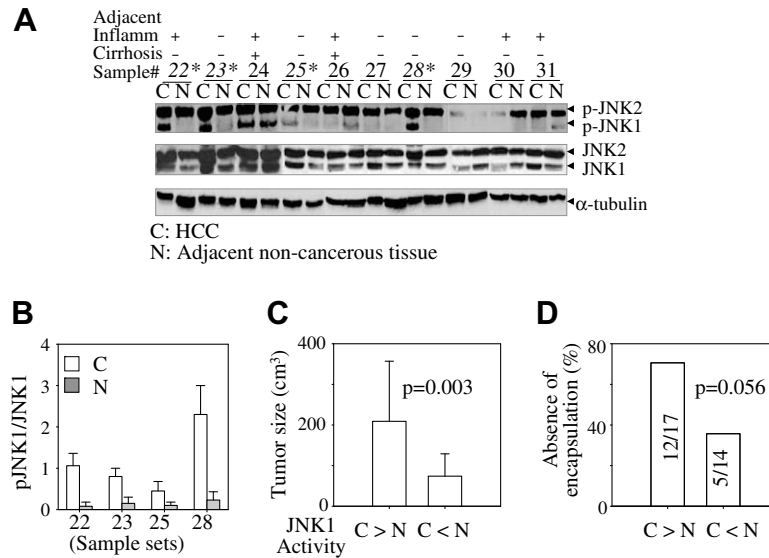


**Fig. 1.** Enhanced JNK1 activation in human HCC. (A) Total protein extracts were prepared from 31 sets of HCC (C) along with the paired ANC tissue (N) and subjected to Western blotting using antibodies against phospho-JNK (p-JNK) and total JNK. The data show representative results from sample pairs 22 to 31. The sample pairs with an increased JNK1 activation (p-JNK1) were indicated with asterisk (\*). The status of inflammation and cirrhosis of the ANC tissues for each pair of samples were indicated with “+” sign on the top of the panel. (B) Quantification of JNK1 activation in HCC(C) vs ANC (N) by densitometry using AlphaEase software. (C) Correlation of JNK1 activation with the tumor sizes. HCC samples were grouped based on JNK1 activation relative to their paired ANC tissues. C > N: JNK1 activation in HCC is higher than that in ANC tissues. Average tumor sizes of the two HCC groups were shown. (D) Absence of encapsulation of the HCC samples with higher (C > N) or lower (C < N) JNK1 activation. The *p*-value was calculated by Fisher’s exact test. Deficiency in tumor encapsulation may be indicative for local invasiveness of the tumors.

we evaluated JNK activation in 31 human HCC tissue samples that were paired with the adjacent non-cancerous tissues by immunoblotting using antibodies against phosphorylated JNK (p-JNK) and total JNK, respectively. While a roughly equal JNK2 activation was observed between HCC and the paired ANC tissue in all of these samples, an increased JNK1 activation could be detected in 17 HCC samples relative to their paired ANC tissues (group 1, C > N, Fig. 1A, the representative data for samples 22–31, and Supplemental Table 1). Fig. 1B shows the ratio of p-JNK vs total JNK between HCC and ANC among sample sets 22, 23, 25, and 28 by densitometry scanning of three independent Western blotting experiments. Among the remaining 14 samples, 12 samples showed a similar activation of JNK1 between HCC and ANC (Supplemental Table 1, group 2, C = N, among which five HCC samples exhibited higher level of total JNK1 and JNK2 proteins), two samples exhibited a decreased JNK1 activation in HCC relative to the ANC (group 3, C < N). The enhanced JNK1 activation, rather than the activation of the alternatively spliced JNK1 or JNK2 isoforms, was confirmed by the use of JNK1-specific antibody that has no cross-reaction with JNK2 (data not shown). The possibility of alternative splicing of JNK1 and JNK2 in the liver tissues was also ruled out by RT-PCR analyses using RNAs extracted from liver tissues and PCR primers that specifically amplify the 3′-terminal 250 nt regions of  $\alpha 1/\beta 1$  and  $\alpha 2/\beta 2$  mRNAs for both JNK1 and JNK2 (data not shown). No significant differ-

ence was noted in the patient data and patho-histological analyses for the ANC tissues among these groups, except for a relatively lower percentage of cirrhosis in the adjacent tissues in group 1 samples (Supplemental Table 1). However, an association between enhanced JNK1 activation and increased tumor sizes was observed (Fig. 1C). Furthermore, the encapsulation is missing in the HCC tissues with higher JNK1 activation relative to the paired ANC tissues, which possibly implies a local invasiveness of the tumors (Fig. 1D).

Previous studies indicated that genetic deficiency in IKK subunits resulted in an enhanced JNK activation in both cell lines and animal models [9,10,19–21]. To determine whether there is an inverse relationship between JNK1 activation and IKK expression, the mRNA levels of IKK $\alpha$ , IKK $\beta$ , and NEMO/IKK $\gamma$  in HCC and the paired ANC tissue was determined by RT-PCR. There appeared to be no defect in the expression of these IKK subunits in the HCC samples that show an enhanced JNK1 activation (data not shown).

### 3.2. Identification of gene expression pattern between HCC and ANC tissues

It has been generally viewed that sustained JNK activation is one of the key driving forces for the expression of genes that are linked to cell cycle transition and cell proliferation, common features of the malignantly transformed cells [11,22]. Accordingly, we next selected five

sets of HCC samples that show either an enhanced JNK1 activation relative to the paired ANC tissues (samples 22, 23, and 28 in Fig. 1A) or an roughly equal level of JNK1 activation between HCC and the paired ANC tissue (samples 26 and 29 in Fig. 1A) for gene expression profiling by microarray using Affymetrix human U133 plus 2 chip containing over 54,000 probe sets for 39,500 human genes. We first compared the general differences in gene expression pattern between all of these HCC samples and the paired ANC tissues. A roughly unified gene

expression pattern was observed in these pairs of HCC samples compared to their respective paired ANC tissues (Fig. 2A). The HCC tissues exhibited a more than 2-fold increase in expression of 1915 genes and a more than 2-fold decreased expression of 499 genes with a *p*-value less than 0.05 (Supplemental Table 2). A false discovery rate (FDR) correction test was also applied to analyze above data for significant changes of gene expression, which showed that more than 60% of these genes with expression changes large than 2-fold passed the  $FDR \leq 0.15$

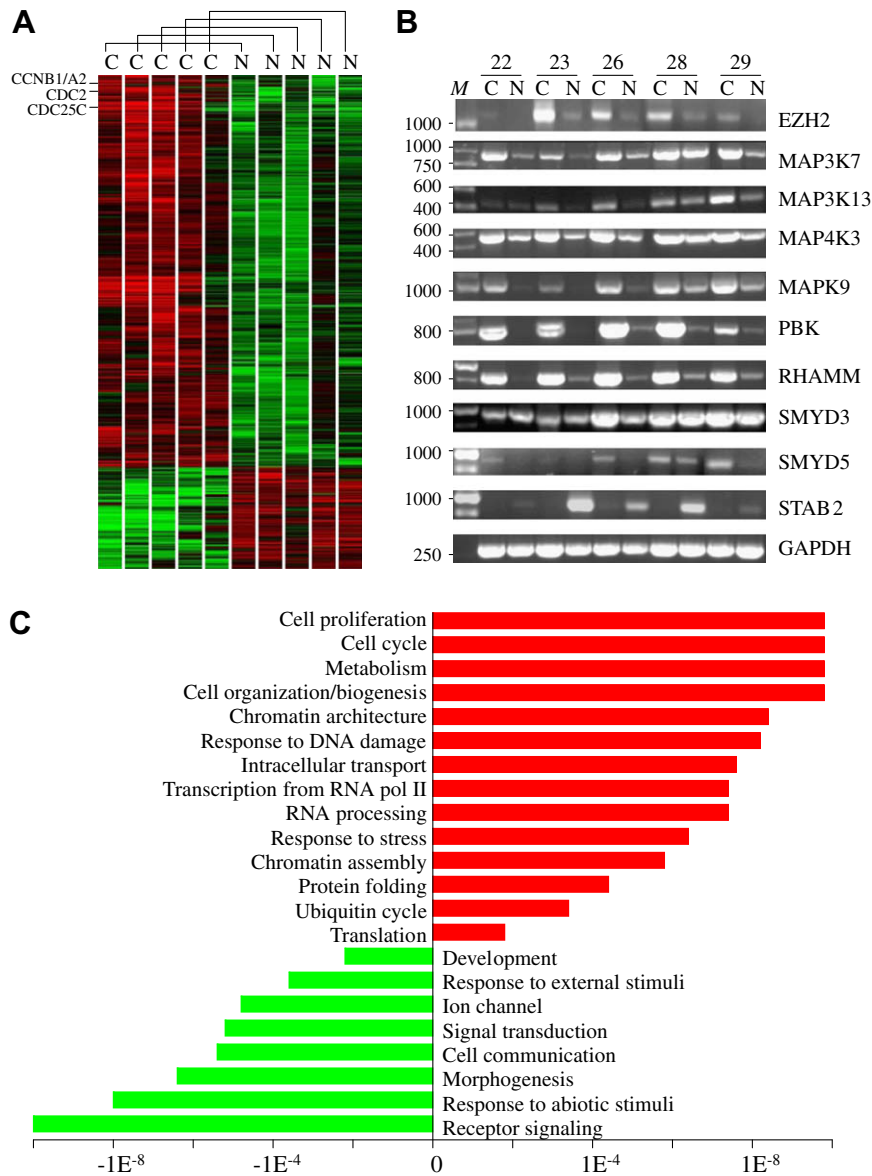


Fig. 2. HCC exhibited increased expression of the genes involved in cell growth, mitosis, biogenesis, metabolism, and RNA transcription. (A) Gene expression profiles of five HCC (C) samples vs their corresponding ANC tissues (N). Data are extracted from microarray using Affymetrix human U133 plus 2 chip containing probes for 39,500 human genes. Red color indicates increased expression of 1915 genes; Green color indicates decreased expression of 499 genes. Genes for CCNB1, CCNA2, CDC2, and CDC25C were indicated on the left of the panel. (B) Verification of the gene expression profiling for the selected genes by RT-PCR. The numbers on the left of each panel indicate sizes of DNA markers. (C) Ontology categories for the genes whose expression level was changed more than 2-fold in HCC. Red color shows increased expression of the genes in HCC as grouped by ontology terms on the left side of the y-axis; Green color shows decreased expressed genes in HCC. The significance as determined by *p*-values was graphed along the x-axis.

threshold (data not shown). The altered expression of these genes was verified by RT-PCR for several randomly selected genes for EZH2, MAP kinase signaling, PDZ binding kinase (PBK), hyaluronan receptor for H-ras-induced cell locomotion (RHAMM) and two proteins involved in histone H3 lysine 4 tri-methylation (SMYD3 and SMYD5) (Fig. 2B). The expression of stabilin2 (STAB2) was nearly undetectable in all of the five HCC samples by RT-PCR, which is consistent with a more than 10-fold decrease in HCC relative to the ANC as demonstrated in gene expression profiling. Further analysis of gene expression profiling data by ontology categories suggested that the highest expressed genes in HCC are those critical for cell proliferation, cell cycle, metabolism, cell organization, and biogenesis (Fig. 2C and Supplemental Table 2), and histone H3 methylation (Supplemental Table 3).

It is intriguing to note that HCC also showed a substantial decrease in the expression of the genes involved in receptor signaling, response to abiotic or external stimuli, morphogenesis, cell communication and signal transduction, ion channel, development, and tumor suppression (Fig. 2C and Supplemental Table 4).

### 3.3. JNK1 activation associates with the regulation of genes involved in cell growth and metabolism in HCC

Emerging evidence suggested a direct link between JNK activation and cell growth and metabolic regulation [23]. To discern relationships between JNK1 activation and alteration of the gene expression patterns that contribute to the increased growth of HCC, the data

of gene expression profiling were re-analyzed by extracting the data from HCC samples only. A re-clustering was made between HCC samples 22, 23, and 28 that exhibit higher JNK1 activation than their paired ANC tissues and HCC samples 26 and 29 that show equal or lower JNK1 activation relative to their corresponding ANC tissues (Fig. 3A). JNK1 activation affected the expression of 1157 genes, of which 446 were up-regulated and 711 were down-regulated (see Supplemental Table 5). Ontology categorization of these genes by Explain tool of the Biological Database [24] suggested that genes for metabolism, electron transport, biosynthesis, cell cycle, and cell death are statistically overexpressed in the HCC samples exhibiting higher JNK1 activation (Fig. 3B). In contrast, the expression of the genes for G-protein receptor signaling, signal transduction, cell communication, development, cell adhesion, morphogenesis, and differentiation were down-regulated in these HCC samples with higher JNK1 activation (Fig. 3B). It is additionally intriguing to note that the genes for all of the p450 family members and the antioxidant enzymes including SOD1, catalase, MGST1, MGST2, GSTK1, AKR7A2, EPHX1, and EPHX2, that are critical for redox regulation and antioxidant responses, are down-regulated in these HCC samples with higher JNK1 activation (Supplemental Tables 6 and 7).

### 3.4. Correlation of JNK1 activation with the elevated levels of histone H3 methylation

In addition to these genes mentioned above, we also noted that several genes that are important for histone

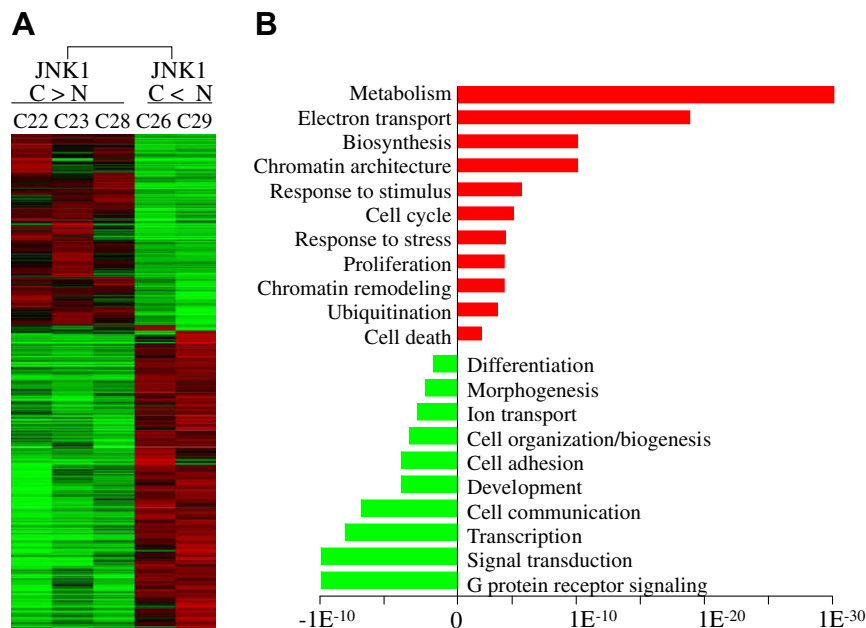
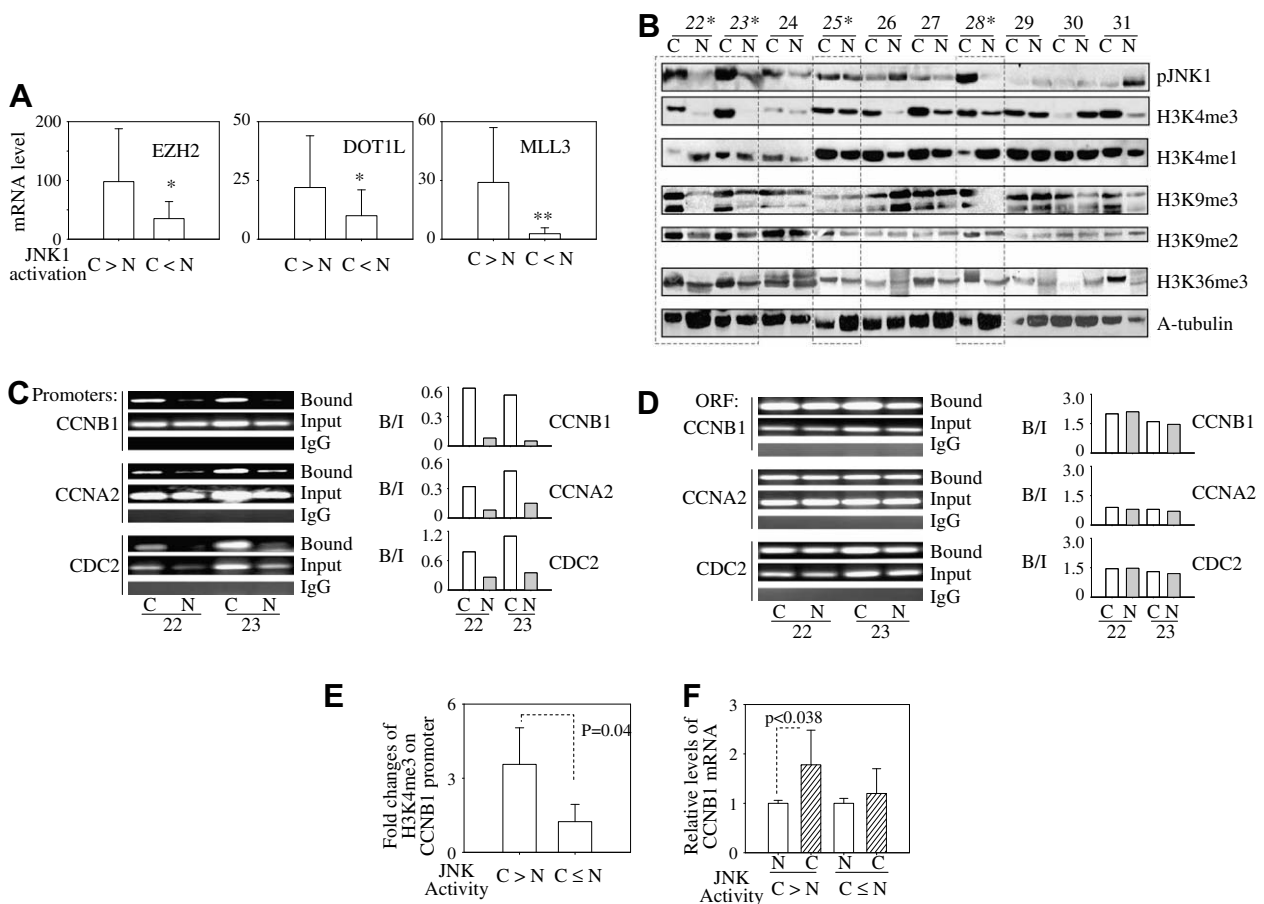


Fig. 3. Comparison of the gene expression profiling between HCC samples showing higher JNK1 activation ( $C > N$ ) and the HCC samples showing lower JNK1 activation ( $C \leq N$ ) relative to their paired ANC tissues. (A) Gene expression profiling of the two groups of HCC samples based on the JNK1 activation. (B) Ontology categories for the genes whose expression level was changed more than 2-fold between two groups of HCC samples.

H3 methylation were highly expressed in the HCC samples that showed higher JNK1 activation as compared to the HCC samples that showed lower JNK1 activation. These genes include EZH2, DOT1L, and MLL3 (Fig. 4A and Supplemental Tables 2 and 3). Both EZH2 and DOT1L are involved in histone H3 lysine 9 and/or 27 methylation, which associated with repression of tumor suppressor genes. The MLL3, on the other hand, is possibly able to induce histone H3 lysine 4 tri-methylation (H3K4me3), leading to active transcription of genes for cell cycle and proliferation [22]. To determine whether the states of histone H3 methylation were altered in HCC and the paired ANC, immunoblot-

ting was performed using antibodies against the different methylation states of histone H3 on lysines 4, 9, and 36 (Fig. 4B). Comparison of the JNK activation state with the histone H3 methylation, as measured by the methylation-specific antibodies, reveals that HCC samples showing higher JNK1 activation relative to their paired ANC tissues are all in the group of samples with increased levels of H3K4me3, H3K9me3, and H3K36me3. In contrast, HCC samples showing equal or lower JNK1 activation relative to the paired ANC tissues are all in the group of samples exhibiting normal level of H3K4me3 and H3K9me3 (Fig. 4B). Such correlation between JNK1 activation and the methylation



**Fig. 4.** JNK1 activation is associated with alterations in histone H3 methylation in HCC. (A) Expression levels of the mRNAs for EZH2, DOT1L and MLL3 in two groups of HCC samples that either show higher JNK1 activation (C > N) or lower JNK1 activation (C ≤ N) relative to their paired non-cancerous tissues. The data were derived from gene profiling using Affymetrix U133 plus 2 chips. \**p* ≤ 0.05; \*\**p* ≤ 0.001. (B) The levels of histone H3 lysine 4 mono- and tri-methylation (H3K4me1 and H3K4me3) were determined by Western blotting using antibodies against H3K4me3 and H3K4me1, respectively. The same membranes were stripped and re-probed with antibodies against H3K9me3, H3K9me2, and H3K36me3, respectively. The dashed-line rectangles indicate HCC samples with higher JNK1 activation relative to their paired non-cancerous tissues. The level of α-tubulin was measured as a loading control for each tissue sample. (C) The level of H3K4me3 occupancy on the promoter region of CCNB1, CCNA2, and CDC2 was determined by ChIP assay using anti-H3K4me3 antibody. The input DNA and immunoprecipitated DNA (bound DNA) were amplified by PCR using primers corresponding to the proximal promoter region of these genes. The relative ratio of the bound DNA (B) vs input DNA (I) was shown on the right for each of the tested gene. (D) The input and bound DNA of H3K4me3 was amplified by PCR using primers corresponding to the open-reading-frame of the tested genes. The bar graphs on the right of each panel show ratio of the bound DNA (B) vs input DNA (I). (E) ChIP assay of H3K4me3 abundance on the CCNB1 promoter in the HCC samples grouped based on the JNK1 activation. Fold changes were calculated by the quantitative ChIP assay of H3K4me3 on CCNB1 promoter in HCCs vs ANC in each group. (F) Expression of mRNA for CCNB1 in HCC samples (C) and their paired ANC tissues (N) are grouped by the levels of JNK1 activation in HCC samples relative to their paired ANC tissues.

states of histone H3 was further confirmed among the remaining HCC samples and the paired ANC tissues (Supplemental Table 8).

A recent study suggested that active gene promoters are enriched in H3K4me3 [25]. It is very likely, thus, that the increased expression of genes in cell growth and cell cycle regulation in HCC where JNK1 is highly activated is associated with the elevated level of H3K4me3. To verify this is indeed the case, we next used chromatin immunoprecipitation (ChIP) to examine the states of H3K4me3 occupancy in the promoter region of cyclin B1 (CCNB1), cyclin A2 (CCNA2), CDC2, and CDC25C. All of these genes were highly expressed in HCC relative to the respective paired ANC tissues as demonstrated in gene profiling (Fig. 2A and Supplemental Table 2), which showed notable correlation with the JNK1 activation status in these HCC samples (Supplemental Table 5). We selected samples 22 and 23, which showed clear enhancement in JNK1 activation (Figs. 1A and 4B) and elevation of H3K4me3 in HCC (Fig. 4B) as compared to their corresponding ANC tissues, for ChIP assay using anti-H3K4me3 antibody. The input and H3K4me3 bound DNA were amplified by sequence-specific PCR using primers corresponding to the respective proximal promoter regions. Notably, we found that the promoters for CCNB1, CCNA2, and CDC2 were highly enriched for H3K4me3 in HCC in both samples (Fig. 4C). In the ANC tissues, only marginal binding of H3K4me3 to the promoters of these genes could be detected. Both input and H3K4me3 bound DNA for CDC25C promoter were poorly amplified in either HCC or the paired ANC and, therefore, the results for this particular gene are inclusive. There was no difference between HCC and the non-cancerous tissues in the H3K4me3 occupancy in the open reading frame (ORF) for all of these genes tested (Fig. 4D). We next compared the abundance of H3K4me3 occupancy on the CCNB1 promoter in the HCC samples showed different JNK1 activation. This analysis suggested that HCC samples with higher JNK1 activation relative to their ANC tissues exhibited a higher abundance of H3K4me3 in the CCNB1 promoter as compared to the HCC samples with lower JNK1 activation relative to their ANC tissues (Fig. 4E). A quantitative RT-PCR analysis confirmed that HCC samples with higher JNK1 activation exhibit increased levels of CCNB1 (Fig. 4F), CCNA2 and CDC2 mRNAs (data not shown).

### 3.5. Deficiency in JNK signaling compromises EZH2 induction

The above data suggested a clear correlation between JNK1 activation and gene expression, such as EZH2, in HCC tissues. Accumulating evidence suggests an abnormal elevation of EZH2 expression during tumorigenesis, such as prostate cancer and breast cancer [26,27]. It is

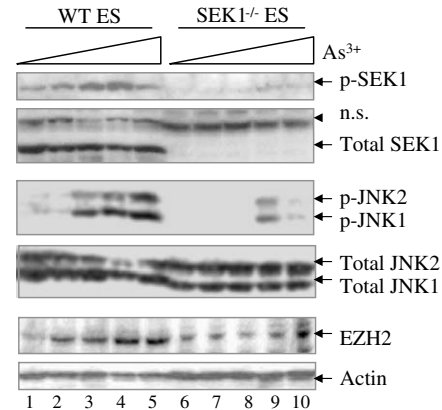


**Fig. 5. Deficiency in JNK signaling compromises EZH2 induction.** Wild-type (WT) ES cells and  $SEK1^{-/-}$  ES cells were cultured in DMEM medium containing 20% FCS and nucleosides (30  $\mu$ M adenosine, 30  $\mu$ M guanosine, 30  $\mu$ M cytidine, 30  $\mu$ M uridine, and 10  $\mu$ M thymidine) in 6-well plates. When the cells form sub-confluence, the cells were treated with 0, 2.5, 5, 10, or 20  $\mu$ M arsenic ( $As^{3+}$ ) for 6 h. Total cell lysates were used for Western blotting using the indicated antibodies.

believed that overexpression of EZH2 provides a proliferative advantage to either primary cells or transformed cells by disrupting the pRb-mediated suppression on the genes for cell cycle regulation [28]. To provide direct evidence showing the role of JNK signaling on the expression of the genes important for the tumorigenic transformation of the cells, we tested the inducibility of EZH2 in embryonic stem cell line (ES) with a genetic disruption of  $SEK1$  ( $JNKK1$ ) gene.  $SEK1$  is a direct upstream kinase for JNK activation in cellular responses to a variety of extracellular and intracellular stress signals [29]. In wild-type (WT) ES cells, arsenic ( $As^{3+}$ ), a previously documented potent JNK activator [19], induced a pronounced activation of JNK (p-JNK) as well as  $SEK1$  (p $SEK1$ ) in a dose-dependent manner (Fig. 5, lanes 1–5, 0, 2.5, 5, 10, and 20  $\mu$ M of  $As^{3+}$ ). In  $SEK1^{-/-}$  ES cells, however, only a marginal activation of JNK could be seen in  $As^{3+}$ -treated cells (Fig. 5, lanes 6–10). The induction of EZH2 was notable in the WT ES cells, which was parallel with the activation of JNK. In contrast, the induction of EZH2 was compromised in the  $SEK1^{-/-}$  ES cells (Fig. 5). Thus, these data suggest that the expression of EZH2 is indeed dependent on JNK signaling, at least partially.

## 4. Discussion

We have investigated the potential roles of JNK1 activation in human HCC and demonstrated a strong association of JNK1 with tumor size and expression of the genes involved in metabolism, cell cycle, and proliferation. We also provide evidence showing that JNK1 activation is responsible, at least partially, for the altered expression of genes in human HCC by affecting the epi-

genetic modifications of the histone H3 protein. Specifically, JNK1 activation up-regulates expression of MLL3, DOT1L and EZH2 that contribute to tri-methylation of lysines 4, 9, 36, and possibly 27 in HCC. The elevated level of H3K4me3 might be directly involved in the increased expression of genes for cell growth regulation, such as CCNB1, CCNA2, and CDC2. JNK1 might also be accountable for the silencing of genes required for differentiation, development, morphogenesis, ion channels, cell-to-cell communication, and tumor suppression.

Human HCC has been generally viewed as a disease with accumulation of genetic alternations that are responsible for the expression of genes controlling cell cycle and cell proliferation [2]. The importance of epigenetic alterations in HCC, however, has been largely unexplored, despite a limited number of reports suggesting hypermethylation of the genes encoding p16(INK4a) [30], E-cadherin [31], target of methylation-induced silencing 1 (TMS1) [32], COX2 [33], and deleted in liver cancer 1 (DLC1) [34] in HCC. It is also unclear whether the changes in the epigenetic landscape of the histone proteins played considerable roles on DNA methylation and the pathogenesis of HCC. The amino-terminal tails of histone H3 and H4 undergo a variety of post-transcriptional modifications, such as phosphorylation, ubiquitination, acetylation, and methylation [35]. The trimethylation of lysine 4 of histone H3 (H3K4me3) and acetylation of lysines 9 and 14 (H3K9ac and H3K14ac) are associated with active transcription of the genes. In contrast, the tri-methylation of lysines 9 and 27 of histone H3 (H3K9me3 and H3K27me3) are acting as inhibitory markers for silencing of gene expression through inducing DNA methylation and the formations of constitutive, facultative, and focal heterochromatins [36].

Compelling evidence suggests that the JNK family kinases are key regulators of gene transcription through AP-1 transcription factors [22], whereas the potential epigenetic modulation of JNK on a broad range of gene expression is currently underemphasized. In *Drosophila*, DFos phosphorylation by JNK is capable of recruiting histone acetyltransferase (HAT), Chameau, leading to histone H4 acetylation and target gene transcription [37]. It is conceivable, therefore, that JNK might be able to promote formation of H3K4me3 through either induction of MLL3 or the facilitation of histone H3 acetylations, or both, which provide a proliferative advantage of the cells. Evidence supporting this was from the observed enrichment of H3K4me3 in the gene promoters and the increased expression of CCNA2, CCNB1 and CDC2, along with other cell proliferative genes, in HCC samples with a higher level of JNK1 activation. The association of JNK1 activation with the enhanced expression of EZH2 and DOT1L, on the other hand, might be critical for the silencing of the differentiation- and development-related genes in the hepatocytes. As an active catalytic

component of polycomb repressive complex 2 (PRC2) for the formation of H3K9me3 and H3K27me3, EZH2 has been previously demonstrated to be an oncogenic protein in prostate cancer [38,39], breast cancer [40], ovarian carcinoma [41], lymphomas [42], gastric cancer [43], and HCC [44–46]. Emerging evidence suggests that EZH2 along with other assembled PRC2 subunits represses expression of the genes required for cell differentiation, lineage development, and tumor suppression through methylations on H3K9, H3K27, and DNA [47–49]. Ontology characterization of the differential expressed genes in the HCC samples with a higher JNK1 activation suggested a significant down-regulation of the genes for G protein receptor signaling, signal transduction, cell–cell communication, cell adhesion, ion transport, development, and differentiation (Fig. 3B). The spectrum of these down-regulated genes is strikingly similar to the de novo methylated genes in the cancer cells [50], which further supports the notion of JNK1 activation and the EZH2-dependent repression of the differentiating genes and tumor suppressors. It is currently unclear how JNK affects the expression or function of EZH2. Our preliminary data suggest that activation of JNK is critical for stress-induced expression of EGR1, a transcription factor important for the transcription of many earlier response genes. Surveying the genomic sequence of the EZH2 gene suggested that there are at least two conserved EGR1 sites located in the proximal promoter and 5'-UTR regions, respectively, of the EZH2 gene. It is very likely, therefore, JNK1 contributes to elevation of the EZH2 level through the EGR1-mediated transcription of the EZH2 gene.

It is intriguing to note an inverse relationship between JNK1 activation and the expression of p450 family members as well as several enzymes important for redox regulation in HCC samples. Both p450 family members and redox regulators are important in metabolism and detoxification of carcinogens. Some types of genetic polymorphisms in p450 genes contribute to HCC susceptibility [51], possibly due to compromised metabolic activity of p450 proteins on carcinogens. An appreciable decrease in the expression of the p450 genes was also noted in HCV-associated HCC [52]. In a mouse hepatocarcinoma model induced by arsenic, the expression of the majority of male-predominant p450 members was decreased [53]. The later observation may be complementary to the present study showing inverse relationship between JNK1 activation and p450 expression, since the fact that arsenic is an established potent inducer for JNK activation in a wide range of cell types [19]. Although it is currently unknown whether JNK signaling and the EZH2/PRC2 directly repress the expression of the p450 genes, promoter CpG DNA methylation of several p450 members had been previously demonstrated either in cancer tissues or cell lines [54–57]. The decreased expression of the redox regulatory enzymes including SOD, catalase, MGSTs,

AKR7A2, and EPHXs may enhance the carcinogenic potential of aflatoxin B1, one of the most common HCC etiologic factors [2]. Genetic studies suggested that patients with some polymorphisms associated with compromised function of these enzymes have an increased risk of developing HCC [58].

The importance of JNK activation or activity in human HCC has not been addressed yet, although few animal studies suggested linkage of JNK activation in chemical carcinogen-induced HCC [10,11]. The association of JNK1 with the epigenetic alternations, mainly the elevation of H3K4me3, H3K9me3, and the expression of EZH2 that is involved in both histone and DNA methylation indicates a pivotal role of JNK on the development of the human HCC. Both environmental and viral carcinogens are capable of activating JNK. As a consequence, genetic and epigenetic signals are altered, leading to a sustained expression of cell proliferative genes and a repression of the genes important for cell differentiation and tumor suppression. Thus, biological or pharmacological intervention on JNK activation may be a plausible new strategy in delaying the initiation and progression of HCC in the high risk population.

#### Acknowledgements

*Grant support:* This research was supported by intramural research grant from the National Institute for Occupational Safety and Health, Centers for Disease Control and Prevention of the USA to F. Chen (70036) and partially supported from F. Chen's personal account. X. Shi was supported by NIH Grants 5R01CA119028 and 5R01CA116697. We are indebted to Dr. Hiroshi Nishina, Department of Physiological Chemistry, Graduate School of Pharmaceutical Sciences, University of Tokyo, for his gift of wild-type and SEK1<sup>-/-</sup> ES cells. We thank the members in the Pathology and Physiology Research Branch of NIOSH for suggestions and critical reading.

#### Appendix A. Supplementary data

Supplementary data associated with this article can be found, in the online version, at [doi:10.1016/j.jhep.2008.07.037](https://doi.org/10.1016/j.jhep.2008.07.037).

#### References

- [1] Llovet JM, Di Bisceglie AM, Bruix J, Kramer BS, Lencioni R, Zhu AX, et al. Design and endpoints of clinical trials in hepatocellular carcinoma. *J Natl Cancer Inst* 2008;100:698–711.
- [2] Farazi PA, DePinho RA. Hepatocellular carcinoma pathogenesis: from genes to environment. *Nat Rev Cancer* 2006;6:674–687.
- [3] Kensler TW, Qian GS, Chen JG, Groopman JD. Translational strategies for cancer prevention in liver. *Nat Rev Cancer* 2003;3:321–329.
- [4] Bruix J, Sherman M, Llovet JM, Beaugrand M, Lencioni R, Burroughs AK, et al. Clinical management of hepatocellular carcinoma. Conclusions of the Barcelona-2000 EASL conference. European Association for the Study of the Liver. *J Hepatol* 2001;35:421–430.
- [5] Llovet JM, Bruix J. Novel advancements in the management of hepatocellular carcinoma in 2008. *J Hepatol* 2008;48:S20–S37.
- [6] Bosch FX, Ribes J, Diaz M, Cleries R. Primary liver cancer: worldwide incidence and trends. *Gastroenterology* 2004;127:S5–S16.
- [7] Zender L, Spector MS, Xue W, Flemming P, Cordon-Cardo C, Silke J, et al. Identification and validation of oncogenes in liver cancer using an integrative oncogenomic approach. *Cell* 2006;125:1253–1267.
- [8] Jia HL, Ye QH, Qin LX, Budhu A, Forgues M, Chen Y, et al. Gene expression profiling reveals potential biomarkers of human hepatocellular carcinoma. *Clin Cancer Res* 2007;13:1133–1139.
- [9] Luedde T, Beraza N, Kotsikoris V, van Loo G, Nenci A, De Vos R, et al. Deletion of NEMO/IKKgamma in liver parenchymal cells causes steatohepatitis and hepatocellular carcinoma. *Cancer Cell* 2007;11:119–132.
- [10] Maeda S, Kamata H, Luo JL, Leffert H, Karin M. IKKbeta couples hepatocyte death to cytokine-driven compensatory proliferation that promotes chemical hepatocarcinogenesis. *Cell* 2005;121:977–990.
- [11] Sakurai T, Maeda S, Chang L, Karin M. Loss of hepatic NF-kappa B activity enhances chemical hepatocarcinogenesis through sustained c-Jun N-terminal kinase 1 activation. *Proc Natl Acad Sci USA* 2006;103:10544–10551.
- [12] Kyriakis JM, Avruch J. pp54 microtubule-associated protein 2 kinase. A novel serine/threonine protein kinase regulated by phosphorylation and stimulated by poly-L-lysine. *J Biol Chem* 1990;265:17355–17363.
- [13] Chen F. MAPK8 (mitogen-activated protein kinase 8). *Atlas Genet Cytogenet Oncol Haematol* 2003; URL: <http://AtlasGeneticsOncology.org/Genes/JNK1ID196.html>.
- [14] Sabapathy K, Hochedlinger K, Nam SY, Bauer A, Karin M, Wagner EF. Distinct roles for JNK1 and JNK2 in regulating JNK activity and c-Jun-dependent cell proliferation. *Mol Cell* 2004;15:713–725.
- [15] Hess P, Pihan G, Sawyers CL, Flavell RA, Davis RJ. Survival signaling mediated by c-Jun NH(2)-terminal kinase in transformed B lymphoblasts. *Nat Genet* 2002;32:201–205.
- [16] Okuda K, Ohtsuki T, Obata H, Tomimatsu M, Okazaki N, Hasegawa H, et al. Natural history of hepatocellular carcinoma and prognosis in relation to treatment. Study of 850 patients. *Cancer* 1985;56:918–928.
- [17] Yu J, Ni M, Xu J, Zhang H, Gao B, Gu J, et al. Methylation profiling of twenty promoter-CpG islands of genes which may contribute to hepatocellular carcinogenesis. *BMC Cancer* 2002;2:29.
- [18] Zhang Y, Bhatia D, Xia H, Castranova V, Shi X, Chen F. Nucleolin links to arsenic-induced stabilization of GADD45alpha mRNA. *Nucleic Acids Res* 2006;34:485–495.
- [19] Chen F, Castranova V, Li Z, Karin M, Shi X. Inhibitor of nuclear factor kappaB kinase deficiency enhances oxidative stress and prolongs c-Jun NH2-terminal kinase activation induced by arsenic. *Cancer Res* 2003;63:7689–7693.
- [20] Chen F, Lu Y, Zhang Z, Vallyathan V, Ding M, Castranova V, et al. Opposite effect of NF-kappa B and c-Jun N-terminal kinase on p53-independent GADD45 induction by arsenite. *J Biol Chem* 2001;276:11414–11419.
- [21] Chen F, Lu Y, Castranova V, Li Z, Karin M. Loss of Ikkbeta promotes migration and proliferation of mouse embryo fibroblast cells. *J Biol Chem* 2006;281:37142–37149.
- [22] Hayakawa J, Mittal S, Wang Y, Korkmaz KS, Adamson E, English C, et al. Identification of promoters bound by c-Jun/

- ATF2 during rapid large-scale gene activation following genotoxic stress. *Mol Cell* 2004;16:521–535.
- [23] Weston CR, Davis RJ. The JNK signal transduction pathway. *Curr Opin Cell Biol* 2007;19:142–149.
- [24] Kel A, Kononova T, Waleev T, Cheremushkin E, Kel-Margoulis O, Wingender E. Composite Module Analyst: a fitness-based tool for identification of transcription factor binding site combinations. *Bioinformatics* 2006;22:1190–1197.
- [25] Heintzman ND, Stuart RK, Hon G, Fu Y, Ching CW, Hawkins RD, et al. Distinct and predictive chromatin signatures of transcriptional promoters and enhancers in the human genome. *Nat Genet* 2007;39:311–318.
- [26] Sellers WR, Loda M. The EZH2 polycomb transcriptional repressor – a marker or mover of metastatic prostate cancer? *Cancer Cell* 2002;2:349–350.
- [27] Cao R, Zhang Y. The functions of E(Z)/EZH2-mediated methylation of lysine 27 in histone H3. *Curr Opin Genet Dev* 2004;14:155–164.
- [28] Tonini T, D'Andrilli G, Fucito A, Gaspa L, Bagella L. Importance of Ezh2 polycomb protein in tumorigenesis process interfering with the pathway of growth suppressive key elements. *J Cell Physiol* 2008;214:295–300.
- [29] Xia Y, Wu Z, Su B, Murray B, Karin M. JNKK1 organizes a MAP kinase module through specific and sequential interactions with upstream and downstream components mediated by its amino-terminal extension. *Genes Dev* 1998;12:3369–3381.
- [30] Wong IH, Lo YM, Zhang J, Liew CT, Ng MH, Wong N, et al. Detection of aberrant p16 methylation in the plasma and serum of liver cancer patients. *Cancer Res* 1999;59:71–73.
- [31] Su PF, Lee TC, Lin PJ, Lee PH, Jeng YM, Chen CH, et al. Differential DNA methylation associated with hepatitis B virus infection in hepatocellular carcinoma. *Int J Cancer* 2007;121:1257–1264.
- [32] Zhang C, Li H, Zhou G, Zhang Q, Zhang T, Li J, et al. Transcriptional silencing of the TMS1/ASC tumour suppressor gene by an epigenetic mechanism in hepatocellular carcinoma cells. *J Pathol* 2007;212:134–142.
- [33] Murata H, Tsuji S, Tsujii M, Sakaguchi Y, Fu HY, Kawano S, et al. Promoter hypermethylation silences cyclooxygenase-2 (Cox-2) and regulates growth of human hepatocellular carcinoma cells. *Lab Invest* 2004;84:1050–1059.
- [34] Wong CM, Lee JM, Ching YP, Jin DY, Ng IO. Genetic and epigenetic alterations of DLC-1 gene in hepatocellular carcinoma. *Cancer Res* 2003;63:7646–7651.
- [35] Reik W. Stability and flexibility of epigenetic gene regulation in mammalian development. *Nature* 2007;447:425–432.
- [36] Regha K, Sloane MA, Huang R, Pauler FM, Warczuk KE, Melikant B, et al. Active and repressive chromatin are interspersed without spreading in an imprinted gene cluster in the mammalian genome. *Mol Cell* 2007;27:353–366.
- [37] Miotto B, Sagnier T, Berenger H, Bohmann D, Pradel J, Graba Y. Chameau HAT and DRpd3 HDAC function as antagonistic cofactors of JNK/AP-1-dependent transcription during *Drosophila* metamorphosis. *Genes Dev* 2006;20:101–112.
- [38] LaTulippe E, Satagopan J, Smith A, Scher H, Scardino P, Reuter V, et al. Comprehensive gene expression analysis of prostate cancer reveals distinct transcriptional programs associated with metastatic disease. *Cancer Res* 2002;62:4499–4506.
- [39] Varambally S, Dhanasekaran SM, Zhou M, Barrette TR, Kumar-Sinha C, Sanda MG, et al. The polycomb group protein EZH2 is involved in progression of prostate cancer. *Nature* 2002;419:624–629.
- [40] Kleer CG, Cao Q, Varambally S, Shen R, Ota I, Tomlins SA, et al. EZH2 is a marker of aggressive breast cancer and promotes neoplastic transformation of breast epithelial cells. *Proc Natl Acad Sci USA* 2003;100:11606–11611.
- [41] Lu C, Bonome T, Li Y, Kamat AA, Han LY, Schmandt R, et al. Gene alterations identified by expression profiling in tumor-associated endothelial cells from invasive ovarian carcinoma. *Cancer Res* 2007;67:1757–1768.
- [42] Dukers DF, van Galen JC, Giroth C, Jansen P, Sewalt RG, Otte AP, et al. Unique polycomb gene expression pattern in Hodgkin's lymphoma and Hodgkin's lymphoma-derived cell lines. *Am J Pathol* 2004;164:873–881.
- [43] Matsukawa Y, Semba S, Kato H, Ito A, Yanagihara K, Yokozaki H. Expression of the enhancer of zeste homolog 2 is correlated with poor prognosis in human gastric cancer. *Cancer Sci* 2006;97:484–491.
- [44] Chen Y, Lin MC, Yao H, Wang H, Zhang AQ, Yu J, et al. Lentivirus-mediated RNA interference targeting enhancer of zeste homolog 2 inhibits hepatocellular carcinoma growth through down-regulation of stathmin. *Hepatology* 2007;46:200–208.
- [45] Chen Y, Lin MC, Wang H, Chan CY, Jiang L, Ngai SM, et al. Proteomic analysis of EZH2 downstream target proteins in hepatocellular carcinoma. *Proteomics* 2007;7:3097–3104.
- [46] Sudo T, Utsunomiya T, Mimori K, Nagahara H, Ogawa K, Inoue H, et al. Clinicopathological significance of EZH2 mRNA expression in patients with hepatocellular carcinoma. *Br J Cancer* 2005;92:1754–1758.
- [47] Bracken AP, Dietrich N, Pasini D, Hansen KH, Helin K. Genome-wide mapping of Polycomb target genes unravels their roles in cell fate transitions. *Genes Dev* 2006;20:1123–1136.
- [48] Schlesinger Y, Straussman R, Keshet I, Farkash S, Hecht M, Zimmerman J, et al. Polycomb-mediated methylation on Lys27 of histone H3 pre-marks genes for de novo methylation in cancer. *Nat Genet* 2007;39:232–236.
- [49] Schwartz YB, Pirrotta V. Polycomb silencing mechanisms and the management of genomic programmes. *Nat Rev Genet* 2007;8:9–22.
- [50] Keshet I, Schlesinger Y, Farkash S, Rand E, Hecht M, Segal E, et al. Evidence for an instructive mechanism of de novo methylation in cancer cells. *Nat Genet* 2006;38:149–153.
- [51] Chen X, Wang H, Xie W, Liang R, Wei Z, Zhi L, et al. Association of CYP1A2 genetic polymorphisms with hepatocellular carcinoma susceptibility: a case-control study in a high-risk region of China. *Pharmacogenet Genomics* 2006;16:219–227.
- [52] Tsunedomi R, Iizuka N, Hamamoto Y, Uchimura S, Miyamoto T, Tamesa T, et al. Patterns of expression of cytochrome P450 genes in progression of hepatitis C virus-associated hepatocellular carcinoma. *Int J Oncol* 2005;27:661–667.
- [53] Xie Y, Liu J, Benbrahim-Tallaa L, Ward JM, Logsdon D, Diwan BA, et al. Aberrant DNA methylation and gene expression in livers of newborn mice transplacentally exposed to a hepatocarcinogenic dose of inorganic arsenic. *Toxicology* 2007;236:7–15.
- [54] Anttila S, Hakkola J, Tuominen P, Elovaara E, Husgafvel-Pursiainen K, Karjalainen A, et al. Methylation of cytochrome P4501A1 promoter in the lung is associated with tobacco smoking. *Cancer Res* 2003;63:8623–8628.
- [55] Ling G, Hauer CR, Gronostajski RM, Pentecost BT, Ding X. Transcriptional regulation of rat CYP2A3 by nuclear factor 1: identification of a novel NFI-A isoform, and evidence for tissue-selective interaction of NFI with the CYP2A3 promoter in vivo. *J Biol Chem* 2004;279:27888–27895.
- [56] Nakajima M, Iwanari M, Yokoi T. Effects of histone deacetylation and DNA methylation on the constitutive and TCDD-inducible expressions of the human CYP1 family in MCF-7 and HeLa cells. *Toxicol Lett* 2003;144:247–256.
- [57] Shi H, Yan PS, Chen CM, Rahmatpanah F, Lofton-Day C, Caldwell CW, et al. Expressed CpG island sequence tag microarray for dual screening of DNA hypermethylation and gene silencing in cancer cells. *Cancer Res* 2002;62:3214–3220.
- [58] Laurent-Puig P, Zucman-Rossi J. Genetics of hepatocellular tumors. *Oncogene* 2006;25:3778–3786.